



Optimal control and bifurcation analysis of a delayed fractional-order SIRS model with general incidence rate and delayed control*

Conghui Xu^a, Yongguang Yu^{b,1}, Guojian Ren^b, Xinhui Si^a

^aSchool of Mathematics and Physics,
University of Science and Technology Beijing,
Beijing 100083, China

^bSchool of Mathematics and Statistics,
Beijing Jiaotong University,
Beijing 100044, China
ygyu@bjtu.edu.cn

Received: August 28, 2023 / **Revised:** March 31, 2024 / **Published online:** July 1, 2024

Abstract. A fractional-order generalized SIRS model considering incubation period is established in this paper for the transmission of emerging pathogens. The corresponding Hopf bifurcation is discussed by selecting time delay as the bifurcation parameter. In order to control the occurrence of Hopf bifurcation and achieve better dynamic behaviors, a delayed feedback control is adopted to the model. Further, the delayed fractional-order optimal control problem (DFOCP) is proposed and discussed. The parameters of the proposed model are identified through the measurement data of coronavirus disease 2019 (COVID-19). Based on the results of parameter identification, the corresponding DFOCP with delayed control is numerically solved.

Keywords: optimal control, bifurcation analysis, fractional-order epidemic model, time delay, COVID-19 pandemic.

1 Introduction

Since ancient times, diseases caused by various pathogens have had a serious impact on human life security and global economic development, such as plague, smallpox, SARS, and the COVID-19 that broke out in the world in 2020. Therefore, analyzing the pathology, transmission trends, and behavioral characteristics of infectious diseases plays an important role in disease control. Specifically, the epidemic model is an important mathematical tool used to discuss the dynamic behaviors of infectious diseases. In 1927,

*This research was supported by the National Natural Science Foundation of China (No. 62173027), the Fundamental Research Funds for the Central Universities (No. FRF-TP-22-104A1), and the China Postdoctoral Science Foundation (No. 2023M740221).

¹Corresponding author.

Kermack and McKendrick proposed the SIR infectious disease model, which divided the population into three compartments: susceptible individuals, infected individuals, and recovered individuals [15]. Subsequently, research on epidemic models has been widely developed [5, 22, 27]. In recent years, public health emergencies caused by the COVID-19 have had a serious impact on the world. In order to effectively describe the spread of such sudden infectious diseases and provide theoretical guidance for epidemic control, a generalized epidemic model is proposed and analyzed in this paper.

The incidence rate is an important function used to characterize the transmission ability of diseases in epidemic models, including bilinear incidence rate [15], saturation incidence rate [5], and various forms of nonlinear incidence rate [26, 30]. In order to enhance the universality of the model established in this paper, a generalized incidence rate is used to describe the spread of infectious diseases. Most existing incidence rates are a special form of this generalized incidence rate. In addition, the incubation period is one of the important reasons for the widespread spread of diseases. Infectious diseases that have caused great harm in history have incubation periods, such as pestis, smallpox, SARS, and COVID-19. Virus carriers are prone to contact and infect susceptible individuals before onset of the disease. In order to effectively characterize the spread of infectious diseases with latent periods, time delay is used to describe the incubation period of diseases.

During the transmission of pathogens, the infectious diseases follow biological genetic characteristics. Infectious diseases that cause major health events often have the characteristic of strong infectivity. The stronger the infectivity, the stronger the correlation between the trend of infectious diseases and historical information. Compared to integer-order epidemic model, the fractional-order epidemic model can effectively characterize the heritability and memory of historical information. In addition, the fractional-order differential equation can make up for the shortcoming that integer-order differential equation cannot fit the experimental data completely. In order to effectively fit the historical data of infectious diseases, fractional-order differential equation are adopted to establish the corresponding epidemic model. Furthermore, the Caputo fractional-order differential equation have properties similar to integer-order differential equation, which can better characterize certain nonlinear relationships and biological phenomena. Analyzing the spread of infectious diseases through the Caputo fractional-order differential equation can more accurately reflect the dynamic behavior of infectious disease. In addition, the integer-order epidemic model can be regarded as a special case of the Caputo fractional-order epidemic model. In [19, 25], the authors found that the Caputo fractional-order epidemic model can better fit and predict the trend of COVID-19 than the corresponding integer-order epidemic model.

Furthermore, a fractional-order epidemic model with general incidence and latency delay is established in this paper. The corresponding dynamic behaviors are analyzed. Bifurcation is an important theory in the dynamic analysis of nonlinear systems, especially, in the qualitative analysis of epidemic models [4, 12, 13, 28, 29]. Selecting time delay as the bifurcation parameter, the Hopf bifurcation of the equilibrium point is discussed. In order to capture the occurrence of Hopf bifurcation, a delayed feedback control is introduced into the model, and the corresponding Hopf bifurcation is analyzed. The delayed feedback

control can improve the stability of the equilibrium point, which is numerically verified in this paper.

In addition, many researches of epidemic model are not combined with real data, which lacks explanations for the effectiveness of model construction. In this paper, the COVID-19 pandemic is taken as an example, and the corresponding measurement data are selected to identify the parameters of the model. Based on the results of parameter identification, the accuracy of the theoretical conclusions is verified numerically.

Reasonable control measures are conducive to controlling the spread of diseases. The optimal control theory is to achieve the best control effect of the pandemic within limited resources. In recent decades, fractional-order optimal control problems (FOCP) have been discussed [2, 3, 9]. Compared to the research on delayed optimal control problems in the sense of ordinary differential equations, there is relatively less research on DFOCP [10, 21]. In addition, few studies have applied DFOCP with delayed control to the emerging epidemic model. Therefore, based on the fractional-order epidemic model proposed in this paper, the DFOCP with delayed control is proposed and discussed. The FBSM is applied to solve the DFOCP with delayed control.

The main contributions of this paper are as follows: (i) Based on the basic SIRS model, a fractional-order epidemic model with latency delay and general incidence rate is established. The effectiveness of the proposed model in describing the trend of sudden outbreaks is verified through the measurement data of COVID-19 pandemic. (ii) A delayed feedback control is adopted to the proposed model, and the corresponding Hopf bifurcation is analyzed. Theoretical analysis and numerical simulation demonstrate that the controlled model exhibits better dynamic behavior. (iii) The DFOCP with delayed control is proposed, and the FBSM method is introduced to numerically solve the corresponding DFOCP. (iv) The parameters of the model are identified based on measurement data of COVID-19 pandemic. Further, the accuracy of the theoretical results is verified, and the corresponding DFOCP is numerically solved.

The structure of this paper is organized as follows. In Section 2, a delayed Caputo fractional-order epidemic model with general incidence rate is established. Some dynamic behaviors of the model established in this paper are analyzed in Section 3. In Section 4, the Hopf bifurcation of the proposed model is discussed. The DFOCP with delayed control is proposed and analyzed in Section 5. In Section 6, the parameters of the model are identified based on measurement data of COVID-19 pandemic. Further, the corresponding DFOCP is numerically solved. In Section 7, the conclusion of this paper is drawn.

2 Preliminaries and model derivation

2.1 Preliminaries

Definition 1. (See [20].) The Caputo fractional-order derivative is given below:

$${}^C D_t^\alpha f(t) = \frac{1}{\Gamma(n-\alpha)} \int_a^t (t-\xi)^{n-\alpha-1} f^{(n)}(\xi) d\xi, \quad n-1 \leq \alpha < n.$$

Definition 2. (See [20].) The Riemann–Liouville fractional-order derivative is given below:

$${}^R D_b^\alpha f(t) = \frac{(-1)^n}{\Gamma(n - \alpha)} \frac{d^n}{dx^n} \int_t^b f(\xi)(\xi - t)^{n-1-\alpha} d\xi,$$

and the Riemann–Liouville fractional-order integral is

$${}^R I_b^\alpha f(t) = \frac{1}{\Gamma(\alpha)} \int_t^b f(t)(\xi - t)^{\alpha-1} d\xi, \quad n - 1 \leq \alpha < n,$$

where $\Gamma(\alpha)$ is gamma function.

2.2 Model derivation

There are many forms of incidence rate due to differences in the types of infectious diseases. Inspired by the work of Li [18], a similar general incidence rate $Sf(I)$ is adopted, which satisfies the following conditions:

- (i) $f(I)$ is a locally Lipschitz function on $[0, \infty)$,
- (ii) $f(0) = 0, f(I) > 0$ for $I > 0$,
- (iii) $\lim_{I \rightarrow 0} f(I)/I = \beta > 0, f(I)/I$ is a continuous and monotone nonincreasing function for $I > 0$.

In addition, the incubation period of infectious diseases is characterized by time delay. Diethelm pointed out that the left-hand sides and right-hand sides of the fractional-order biological models should have the same dimensions [7]. The left-hand side of the Caputo fractional-order model have the dimension of $(\text{time})^{-\alpha}$, and it is necessary to ensure that the parameters of the right-hand side of the model also have the same dimension. Therefore, a delayed Caputo fractional-order epidemic model with general incidence is established as follows:

$$\begin{aligned} {}^C D_t^\alpha S(t) &= \Lambda^\alpha S(t) \left(1 - \frac{S(t)}{K}\right) - S(t)f(I) + b_1^\alpha I(t) + b_2^\alpha R(t), \\ {}^C D_t^\alpha I(t) &= S(t - \tau)f(I(t - \tau)) - (r^\alpha + b_1^\alpha + d_1^\alpha + d_2^\alpha)I(t), \\ {}^C D_t^\alpha R(t) &= r^\alpha I(t) - (d_1^\alpha + b_2^\alpha)R(t), \end{aligned} \tag{1}$$

where $S(t) = \phi_1(t) \geq 0$ for $t \in [-\tau, 0], I(t) = \phi_2(t) \geq 0$ for $t \in [-\tau, 0], R(0) = R_0, S(t), I(t),$ and $R(t)$ represent the population size of susceptible individuals, infected individuals, and recovered individuals at time t , respectively, Λ is the recruitment rate of susceptible individuals, K represents the environmental capacity, b_1 and b_2 denote the self-healing rate of infected individuals and immune loss rate, respectively, d_1 and d_2 are the natural death rate and the death rate caused by diseases, respectively.

In order to achieve better dynamical behaviors, a class of bifurcation controller is adopted to model (1). Inspired by the works of Huang [12, 13], a delayed feedback

controller is applied to model (1), which can be expressed as

$$p(t) = \sigma(S(t) - S(t - \tau)),$$

where σ is feedback gain, τ denotes the time delay of feedback control. Further, the corresponding model (1) with delayed feedback controller can be expressed as

$$\begin{aligned} {}^C_0D_t^\alpha S(t) &= \Lambda^\alpha S(t) \left(1 - \frac{S(t)}{K}\right) - S(t)f(I) + b_1^\alpha I(t) + b_2^\alpha R(t) \\ &\quad + \sigma(S(t) - S(t - \tau)), \\ {}^C_0D_t^\alpha I(t) &= S(t - \tau)f(I(t - \tau)) - (r^\alpha + b_1^\alpha + d_1^\alpha + d_2^\alpha)I(t), \\ {}^C_0D_t^\alpha R(t) &= r^\alpha I(t) - (d_1^\alpha + b_2^\alpha)R(t), \end{aligned} \quad (2)$$

where the initial condition is the same as model (1).

Remark 1. If $\sigma = 0$, then the feedback controller $p(t) = \sigma(S(t) - S(t - \tau))$ is invalid in model (2). In epidemiology, feedback controller $p(t)$ can be represented as the self-protection measures for susceptible individuals, including wearing masks and home isolation. When the number of susceptible individuals exposed to the environment is higher than the previous moment, the number of susceptible individuals exposed to the environment can be appropriately reduced by adjusting the self-feedback coefficient σ to avoid the further spread of infectious diseases.

3 Qualitative analysis

Some dynamic behaviors of model (1) are analyzed in this section. Obviously, for initial value $(S_0, I_0, R_0) \in \mathbb{R}_+^3$, there exists a unique solution of model (1) [14, 20].

3.1 Nonnegativity

Theorem 1. For any initial value $(S_0, I_0, R_0) \in \mathbb{R}_+^3$, the solutions of model (1) are nonnegative.

Proof. Let t_1, t_2 , and t_3 be the critical times when $S(t)$, $I(t)$, and $R(t)$ first reach zero and become negative at the next moment, respectively. Let $t_2 = t_3 = \min\{t_1, t_2, t_3\} \neq \infty$, then there exists a sufficiently small $0 < \epsilon < \tau$ with $S(t - \tau) > 0$ and $I(t), R(t) < 0$ in the interval $(t_2, t_2 + \epsilon)$. According to model (1), it can be obtained that

$${}^C_0D_t^\alpha (I + R) \geq -d_1^\alpha (I + R), \quad t \in (t_2, t_2 + \epsilon).$$

According to the fractional-order comparison theorem [24], one has

$$I + R \geq (I_0 + R_0)E_\alpha(-d_1^\alpha t^\alpha) \geq 0, \quad t \in (t_2, t_2 + \epsilon).$$

The above formula contradicts the assumption, which means that $I(t)$ and $R(t)$ cannot simultaneously reach the zero axis before $S(t)$ and become negative at the next moment.

Assuming that $t_3 = \min\{t_1, t_2, t_3\} \neq \infty$, there exists a sufficiently small $\epsilon > 0$ with $I(t) > 0$ and $R(t) < 0$ in the interval $(t_3, t_3 + \epsilon)$. According to model (1), it can be seen that

$${}_0^C D_t^\alpha R \geq -(d_1^\alpha + b_2^\alpha)R, \quad t \in (t_3, t_3 + \epsilon).$$

Similarly, it can be obtained that $R(t) \geq 0$ for $t \in (t_3, t_3 + \epsilon)$, which contradicts the assumption. Therefore, $R(t)$ cannot first reach the zero axis and become negative at the next moment.

Further, assuming that $t_2 = \min\{t_1, t_2, t_3\} \neq \infty$, there exists a sufficiently small $0 < \epsilon < \tau$ with $S(t - \tau) > 0$, $I(t - \tau) > 0$, and $I(t) < 0$ in the interval $(t_2, t_2 + \epsilon)$. Similarly, it can be obtained that $I(t)$ cannot first reach the zero axis and become negative at the next moment.

Assume that $t_1 = \min\{t_1, t_2, t_3\} \neq \infty$. The above analysis has shown that $I(t)$ and $R(t)$ cannot reach and cross the zero axis in finite time. Therefore, the assumption $t_1 = \min\{t_1, t_2, t_3\} \neq \infty$ means that $t_1 \neq t_2$ and $t_1 \neq t_3$. Similarly, it can be obtained that $S(t)$ cannot reach zero for the first time and become negative at the next moment.

Therefore, $S(t)$, $I(t)$, and $R(t)$ cannot reach zero in a finite time and become negative at the next moment. For any initial values $(S_0, I_0, R_0) \in \mathbb{R}_+^3$, the solutions of model (1) are nonnegative. □

3.2 Existence of equilibria

The basic reproduction number \mathcal{R}_0 is established to analyze the existence of equilibria [11, 23]. Obviously, there exists a zero equilibrium $E_0 = (0, 0, 0)$ and a disease-free equilibrium $E_1 = (K, 0, 0)$ in model (1). Therefore, the basic reproduction number can be calculated as

$$\mathcal{R}_0 = \frac{Kf'(0)}{r^\alpha + b_1^\alpha + d_1^\alpha + d_2^\alpha}.$$

Theorem 2. *Model (1) clearly has a zero equilibrium $E_0 = (0, 0, 0)$ and a disease-free equilibrium $E_1 = (K, 0, 0)$. There exists a unique endemic equilibrium $E^* = (S^*, I^*, R^*)$ for model (1) if the condition $1 < \mathcal{R}_0 \leq 2$ holds.*

Proof. Assuming that $E^* = (S^*, I^*, R^*)$ is the endemic equilibrium of model (1), it can be obtained that

$$R^* = \frac{r^\alpha I^*}{b_2^\alpha + d_1^\alpha}, \quad S^* = (r^\alpha + b_1^\alpha + d_1^\alpha + d_2^\alpha) \frac{I^*}{f(I^*)}. \tag{3}$$

Further, one has

$$\frac{\Lambda^\alpha I^*}{f(I^*)} (r^\alpha + b_1^\alpha + d_1^\alpha + d_2^\alpha) \left(1 - \frac{S^*}{K}\right) - \left(d_1^\alpha + d_2^\alpha + \frac{r^\alpha d_1^\alpha}{b_2^\alpha + d_1^\alpha}\right) I^* = 0.$$

Thus, it can be found that I^* is the positive root of the following equation:

$$G(I) = \alpha_1 g(I) [1 - \alpha_2 g(I)] - \left(d_1^\alpha + d_2^\alpha + \frac{r^\alpha d_1^\alpha}{b_2^\alpha + d_1^\alpha}\right) I = 0,$$

where $\alpha_1 = \Lambda^\alpha(r^\alpha + b_1^\alpha + d_1^\alpha + d_2^\alpha)$, $\alpha_2 = (r^\alpha + b_1^\alpha + d_1^\alpha + d_2^\alpha)/K$, and $g(I) = I/f(I)$. The condition $\mathcal{R}_0 > 1$ is established, which can ensure that $G(0) > 0$. Further, one has

$$G'(I) = \alpha_1 g'(I) [1 - 2\alpha_2 g(I)] - \left(d_1^\alpha + d_2^\alpha + \frac{r^\alpha d_1^\alpha}{b_2^\alpha + d_1^\alpha} \right).$$

Obviously, one has $g'(I) \geq 0$ and $g(I) \geq g(0)$. If $\mathcal{R}_0 \leq 2$, it can be obtained that $G'(I) < 0$. Therefore, if $1 < \mathcal{R}_0 \leq 2$, $G(I)$ has a unique positive root on $I \in [0, \infty)$ denoted by I^* . Further, according to formula (3), it can be found that model (1) has a unique endemic equilibrium. \square

3.3 Stability analysis of equilibria

The local asymptotic stability of the disease-free equilibrium E_1 and endemic equilibrium E^* of model (1) is analyzed in this section.

Theorem 3. *With respect to the stability of the disease-free equilibrium E_1 of model (1), the following conclusions are drawn.*

- (i) *The disease-free equilibrium E_1 is asymptotically stable for $\tau = 0$ if the condition $\mathcal{R}_0 < 1$ holds.*
- (ii) *The disease-free equilibrium E_1 is asymptotically stable for $\tau \geq 0$ if the condition $\mathcal{R}_0 < 1$ holds.*

Proof. According to [17], the corresponding characteristic equation of model (1) at E_1 is

$$D(\lambda) = \lambda^{3\alpha} + m_1 \lambda^{2\alpha} + m_2 \lambda^\alpha + m_3 \lambda^{2\alpha} e^{-\lambda\tau} + m_4 \lambda^\alpha e^{-\lambda\tau} + m_5 e^{-\lambda\tau} + m_6 = 0, \tag{4}$$

where

$$\begin{aligned}
m_1 &= \Lambda^\alpha + r^\alpha + b_1^\alpha + b_2^\alpha + 2d_1^\alpha + d_2^\alpha, \\
m_2 &= (b_2^\alpha + d_1^\alpha)(\Lambda^\alpha + r^\alpha + b_1^\alpha + d_1^\alpha + d_2^\alpha) + \Lambda^\alpha(r^\alpha + b_1^\alpha + d_1^\alpha + d_2^\alpha), \\
m_3 &= -Kf'(0), \quad m_4 = -Kf'(0)(\Lambda^\alpha + d_1^\alpha + b_2^\alpha), \\
m_5 &= -\Lambda^\alpha Kf'(0)(b_2^\alpha + d_1^\alpha), \quad m_6 = \Lambda^\alpha(b_2^\alpha + d_1^\alpha)(r^\alpha + b_1^\alpha + d_1^\alpha + d_2^\alpha).
\end{aligned}$$

For $\tau = 0$, substituting $s = \lambda^\alpha$ into characteristic equation (4) yields

$$L(s) = s^3 + l_1 s^2 + l_2 s + l_3 = 0,$$

where $l_1 = m_1 + m_3$, $l_2 = m_2 + m_4$, and $l_3 = m_5 + m_6$. Assume that s_1, s_2 , and s_3 are the roots of characteristic equation $L(s) = 0$. Furthermore, it can be seen that all roots of the characteristic equation $L(s) = 0$ satisfy $|\arg(s_i)| > \pi/2 > \alpha\pi/2$ ($i = 1, 2, 3$) if conditions $l_1 > 0, l_3 > 0$, and $l_1 l_2 > l_3$ hold. Through calculation, it can be concluded that

$$\begin{aligned}
l_1 l_2 - l_3 &= l_1 (\Lambda^\alpha + b_2^\alpha + d_1^\alpha) (r^\alpha + b_1^\alpha + d_1^\alpha + d_2^\alpha) (1 - \mathcal{R}_0) \\
&\quad + \Lambda^\alpha (\Lambda^\alpha + b_2^\alpha + d_1^\alpha) (b_2^\alpha + d_1^\alpha).
\end{aligned}$$

According to the above equations, if $\mathcal{R}_0 < 1$, there are $l_1 > 0, l_3 > 0$, and $l_1 l_2 > l_3$. Therefore, based on the results in [17], the disease-free equilibrium E_1 of model (1) is locally asymptotically stable for $\tau = 0$ under the condition $\mathcal{R}_0 < 1$.

For $\tau > 0$, we assume that $D(\lambda) = 0$ has a pure imaginary root, which can be denoted by $\lambda = \omega i$. Substitute $\lambda = \omega i$ into the characteristic equation (4), and then separate the real and imaginary parts to obtain

$$a_1 \cos(\omega\tau) + a_2 \sin(\omega\tau) = -a_3, \quad a_2 \cos(\omega\tau) - a_1 \sin(\omega\tau) = -a_4,$$

where

$$\begin{aligned} a_1 &= m_3\omega^{2\alpha} \cos(\alpha\pi) + m_4\omega^\alpha \cos \frac{\alpha\pi}{2} + m_5, \\ a_2 &= m_3\omega^{2\alpha} \sin(\alpha\pi) + m_4\omega^\alpha \sin \frac{\alpha\pi}{2}, \\ a_3 &= m_6 + \omega^{3\alpha} \cos \frac{3\alpha\pi}{2} + m_1\omega^{2\alpha} \cos(\alpha\pi) + m_2\omega^\alpha \cos \frac{\alpha\pi}{2}, \\ a_4 &= \omega^{3\alpha} \sin \frac{3\alpha\pi}{2} + m_1\omega^{2\alpha} \sin(\alpha\pi) + m_2\omega^\alpha \sin \frac{\alpha\pi}{2}. \end{aligned}$$

Further calculations allow us to obtain that

$$F(\omega) = \omega^{6\alpha} + f_1\omega^{5\alpha} + f_2\omega^{4\alpha} + f_3\omega^{3\alpha} + f_4\omega^{2\alpha} + f_5\omega^\alpha + f_6 = 0,$$

where

$$\begin{aligned} f_1 &= 2m_1 \cos \frac{\alpha\pi}{2}, & f_2 &= 2m_2 \cos(\alpha\pi) + m_1^2 - m_3^2, \\ f_3 &= 2m_6 \cos \frac{3\alpha\pi}{2} + 2(m_1m_2 - m_3m_4) \cos \frac{\alpha\pi}{2}, \\ f_4 &= m_2^2 - m_4^2 + 2(m_1m_6 - m_3m_5) \cos(\alpha\pi), \\ f_5 &= 2(m_2m_6 - m_4m_5) \cos \frac{\alpha\pi}{2}, & f_6 &= m_6^2 - m_5^2. \end{aligned}$$

Note that $f_1 > 0$, $F(\omega) = 0$ has no positive root if the condition $f_i > 0$ ($i = 2, 3, 4, 5, 6$) hold, which contradicts the assumption. Then one has

$$f_2 > \Lambda^{2\alpha} + (b_2^\alpha + d_1^\alpha)^2 + (r^\alpha + b_1^\alpha + d_1^\alpha + d_2^\alpha)^2(1 - \mathcal{R}_0^2).$$

Therefore, if the condition $\mathcal{R}_0 < 1$ holds, it means that $f_2 > 0$. For convenience, let $\theta_1 = b_2^\alpha + d_1^\alpha$ and $\theta_2 = r^\alpha + b_1^\alpha + d_1^\alpha + d_2^\alpha$. Through calculation, it can be concluded that

$$\begin{aligned} f_3 &= 2 \cos \frac{\alpha\pi}{2} [\theta_2(\Lambda^{2\alpha} + \theta_1^2) + \theta_2^2(\Lambda^\alpha + \theta_1)(1 - \mathcal{R}_0^2) + 3\Lambda^\alpha\theta_1(\Lambda^\alpha + \theta_1)] \\ &\quad + 8\Lambda^\alpha\theta_1\theta_2 \cos^3 \frac{\alpha\pi}{2}. \end{aligned}$$

Since $\alpha \in (0, 1)$, if $\mathcal{R}_0 < 1$ holds, one has $f_3 > 0$. Through calculation, it can be found that

$$m_1m_6 - m_3m_5 = \Lambda^\alpha\theta_1\theta_2^2(1 - \mathcal{R}_0^2) + \Lambda^\alpha\theta_1\theta_2(\Lambda^\alpha + \theta_1).$$

According to the above equation, it can be obtained that $m_1m_6 - m_3m_5 > 0$ if the condition $\mathcal{R}_0 < 1$ holds. Therefore, it can be calculated that

$$f_4 > \Lambda^{2\alpha}\theta_1^2 + (\Lambda^{2\alpha} + \theta_1^2)\theta_2^2(1 - \mathcal{R}_0^2).$$

Hence, if the condition $\mathcal{R}_0 < 1$ holds, one has $f_4 > 0$. By calculation, it can be concluded that

$$m_2m_6 - m_4m_5 = \Lambda^{2\alpha}\theta_1^2\theta_2 + \Lambda^\alpha\theta_1\theta_2^2(\Lambda^\alpha + \theta_1)(1 - \mathcal{R}_0^2).$$

Therefore, if the condition $\mathcal{R}_0 < 1$ holds, one has $f_5 > 0$. Then it can be calculated that

$$f_6 = \Lambda^{2\alpha}\theta_1^2\theta_2^2(1 - \mathcal{R}_0^2).$$

Therefore, it can be obtained that $f_6 > 0$ if the condition $\mathcal{R}_0 < 1$ holds.

In summary, we can obtain that $f_i > 0$ ($i = 2, 3, 4, 5, 6$) if condition $\mathcal{R}_0 < 1$ holds. Therefore, based on the results in [6], $D(\lambda) = 0$ has no pure imaginary roots for all $\tau > 0$ if condition $\mathcal{R}_0 < 1$ holds. The proof of Theorem 3 is completed. \square

Theorem 4. *With respect to the stability of the endemic equilibrium E^* of model (1), the following conclusions are drawn:*

- (i) *The endemic equilibrium E^* is asymptotically stable for $\tau = 0$ if the condition $1 < \mathcal{R}_0 \leq 2$ holds.*
- (ii) *The endemic equilibrium point E^* is asymptotically stable for $\tau \geq 0$ if the condition $1 < \mathcal{R}_0 \leq 2$ holds.*

Proof. The characteristic equation of model (1) at point E^* is

$$H(\lambda) = \lambda^{3\alpha} + h_1\lambda^{2\alpha} + h_2\lambda^\alpha + h_3\lambda^{2\alpha}e^{-\lambda\tau} + h_4\lambda^\alpha e^{-\lambda\tau} + h_5e^{-\lambda\tau} + h_6 = 0, \quad (5)$$

where

$$\begin{aligned} h_1 &= -(n_{11} + n_{22} + n_{33}), & h_2 &= n_{11}n_{22} + n_{22}n_{33} + n_{11}n_{33}, \\ h_3 &= -p_{22}, & h_4 &= (n_{11} + n_{33})p_{22} - n_{12}p_{21}, \\ h_5 &= n_{12}n_{33}p_{21} - n_{11}n_{33}p_{22} - n_{13}n_{32}p_{21}, & h_6 &= -n_{11}n_{22}n_{33} \end{aligned}$$

with

$$\begin{aligned} n_{11} &= \Lambda^\alpha - \frac{2\Lambda^\alpha S^*}{K} - f(I^*), & n_{12} &= b_1^\alpha - S^* f'(I^*), & n_{13} &= b_2^\alpha, \\ n_{22} &= -(r^\alpha + b_1^\alpha + d_1^\alpha + d_2^\alpha), & n_{32} &= r^\alpha & n_{33} &= -(b_2^\alpha + d_1^\alpha), \\ & & p_{21} &= f(I^*), & p_{22} &= S^* f'(I^*). \end{aligned}$$

For $\tau = 0$, substituting $s = \lambda^\alpha$ into (5) yields $K(s) = s^3 + k_1s^2 + k_2s + k_3 = 0$ where $k_1 = h_1 + h_3$, $k_2 = h_2 + h_4$, and $k_3 = h_5 + h_6$. Since $f(I)/I$ is a monotone nonincreasing function, it holds that $f(I) \geq f'(I)I$. Then we have $S^*/K \geq 1/\mathcal{R}_0$ and $1 - f'(I^*)I^*/f(I^*) \geq 0$. Further simplifying the conditions $k_1 > 0$, $k_3 > 0$, and $k_1k_2 > k_3$, it can be obtained that

$$k_1 \geq \Lambda^\alpha \left(\frac{2}{\mathcal{R}_0} - 1 \right) + f(I^*) + b_2^\alpha + d_1^\alpha.$$

If the condition $\mathcal{R}_0 \leq 2$ holds, then one has $k_1 > 0$. For convenience, let

$$\begin{aligned} \theta_1 &= b_2^\alpha + d_1^\alpha, & \theta_2 &= r^\alpha + b_1^\alpha + d_1^\alpha + d_2^\alpha, & \theta_3 &= r^\alpha + b_2^\alpha + 2d_1^\alpha + d_2^\alpha, \\ \varphi_1 &= \frac{2}{\mathcal{R}_0} - 1, & \varphi_2 &= 1 - \frac{f'(I^*)I^*}{f(I^*)}, & \varphi_3 &= 1 - \left(\frac{f'(I^*)I^*}{f(I^*)} \right)^2. \end{aligned}$$

Further, it can be obtained through calculation that

$$k_2 \geq \Lambda^\alpha \varphi_1 (\theta_2 \varphi_2 + \theta_1) + \theta_1 \theta_2 \varphi_2 + \theta_3 f(I^*).$$

Therefore, if $\mathcal{R}_0 \leq 2$ holds, one has $k_2 > 0$. Further, one can calculate that

$$k_3 \geq \Lambda^\alpha \theta_1 \theta_2 \varphi_1 \varphi_2 + (\theta_1 (\theta_2 - b_1^\alpha) - r^\alpha b_2^\alpha) f(I^*).$$

If the condition $\mathcal{R}_0 \leq 2$ holds, one has $k_3 > 0$. Further, it can be calculated that

$$k_1 k_2 - k_3 = \phi_1 \left(\frac{\phi_2}{\theta_1} + \phi_3 + \theta_3 f(I^*) \right) + \theta_1 \phi_3 + (\theta_1^2 + r^\alpha b_2^\alpha) f(I^*),$$

where $\phi_1 = \Lambda^\alpha (2S^*/K - 1) + f(I^*) + \theta_2 \varphi_2$, $\phi_2 = \Lambda^\alpha \theta_1 \theta_2 (2S^*/K - 1) \varphi_2$, $\phi_3 = \Lambda^\alpha \theta_1 (2S^*/K - 1) + \theta_1 \theta_2 \varphi_2$. Therefore, it can be obtained that $k_1 k_2 > k_3$, if the condition $\mathcal{R}_0 \leq 2$ holds.

For $\tau > 0$, assuming that $\lambda = \omega i = \omega (\cos(\pi/2) + i \sin(\pi/2))$ is a pure imaginary root of $H(\lambda) = 0$, then substituting $\lambda = \omega i$ into $H(\lambda) = 0$ and separating the real and imaginary parts, one has

$$c_1 \cos(\omega\tau) + c_2 \sin(\omega\tau) = -c_3, \quad c_2 \cos(\omega\tau) - c_1 \sin(\omega\tau) = -c_4, \tag{6}$$

where

$$\begin{aligned} c_1 &= h_3 \omega^{2\alpha} \cos(\alpha\pi) + h_4 \omega^\alpha \cos \frac{\alpha\pi}{2} + h_5, \\ c_2 &= h_3 \omega^{2\alpha} \sin(\alpha\pi) + h_4 \omega^\alpha \sin \frac{\alpha\pi}{2}, \\ c_3 &= h_6 + \omega^{3\alpha} \cos \frac{3\alpha\pi}{2} + h_1 \omega^{2\alpha} \cos(\alpha\pi) + h_2 \omega^\alpha \cos \frac{\alpha\pi}{2}, \\ c_4 &= \omega^{3\alpha} \sin \frac{3\alpha\pi}{2} + h_2 \omega^\alpha \sin \frac{\alpha\pi}{2} + h_1 \omega^{2\alpha} \sin(\alpha\pi). \end{aligned}$$

Therefore, it can be observed that ω is the positive root of the following equation:

$$W(\omega) = \omega^{6\alpha} + g_1 \omega^{5\alpha} + g_2 \omega^{4\alpha} + g_3 \omega^{3\alpha} + g_4 \omega^{2\alpha} + g_5 \omega^\alpha + g_6 = 0, \tag{7}$$

where

$$\begin{aligned} g_1 &= 2h_1 \cos \frac{\alpha\pi}{2}, \quad g_2 = 2h_2 \cos(\alpha\pi) + h_1^2 - h_3^2, \\ g_3 &= 2(h_1 h_2 - h_3 h_4) \cos \frac{\alpha\pi}{2} + 2h_6 \cos \frac{3\alpha\pi}{2}, \\ g_4 &= h_2^2 - h_4^2 + 2(h_1 h_6 - h_3 h_5) \cos(\alpha\pi), \\ g_5 &= 2(h_2 h_6 - h_4 h_5) \cos \frac{\alpha\pi}{2}, \quad g_6 = h_6^2 - h_5^2. \end{aligned}$$

Since $g_1 > 0$ is satisfied, $W(\omega) = 0$ has no positive root under conditions $g_i > 0$ ($i = 2, 3, 4, 5, 6$), which contradicts the assumption. Further, one has

$$g_2 \geq (f(I^*) + \Lambda^\alpha \varphi_1)^2 + \theta_2^2 \varphi_3 + (\theta_1 + \theta_2) (f(I^*) + \theta_1 + \Lambda^\alpha \varphi_1).$$

It can be found from the above equation that if $\mathcal{R}_0 \leq 2$ holds, one has $g_2 > 0$. Therefore, the condition $g_2 > 0$ can be replaced by the condition $\mathcal{R}_0 \leq 2$. Similarly, one can deduce that

$$g_3 \geq 2 \cos \frac{\alpha\pi}{2} [\varphi_3 \theta_2^2 (\Lambda^\alpha \varphi_1 + \theta_1) + \theta_2 ((f(I^*) + \Lambda^\alpha \varphi_1)^2 + \theta_1^2) + (\theta_2 - b_1^\alpha) \theta_2 + \theta_1 (f(I^*) + \Lambda^\alpha \varphi_1) (f(I^*) + \Lambda^\alpha \varphi_1 + \theta_1)] + 8\theta_1 \theta_2 (f(I^*) + \Lambda^\alpha \varphi_1) \cos^3 \frac{\alpha\pi}{2}.$$

Therefore, if the condition $\mathcal{R}_0 \leq 2$ holds, we have $g_3 > 0$. Further, it can be calculated that

$$h_1 h_6 - h_3 h_5 \geq (f(I^*) + \Lambda^\alpha \varphi_1) (f(I^*) + \Lambda^\alpha \varphi_1 + \theta_1) \theta_1 \theta_2 + \Lambda^\alpha \varphi_1 \varphi_3 \theta_1 \theta_2^2 + \theta_2 (\theta_1 (d_1^\alpha + d_2^\alpha) + r^\alpha d_1^\alpha) f(I^*) + \theta_2 (b_1^\alpha \theta_1 + r^\alpha b_2^\alpha) \varphi_2.$$

If condition $\mathcal{R}_0 \leq 2$ holds, it can be obtained that $h_1 h_6 - h_3 h_5 > 0$. Therefore, under the condition $\mathcal{R}_0 \leq 2$, it can be further calculated that

$$g_4 \geq \varphi_3 \theta_2^2 (\Lambda^{2\alpha} \varphi_1^2 + \theta_1^2) + 2\theta_2 \varphi_1 \Lambda^\alpha f(I^*) (\theta_2 - b_1^\alpha) + \Lambda^\alpha \theta_1^2 (\Lambda^\alpha \varphi_1^2 + 2f(I^*) \varphi_1) + 2b_1^\alpha \Lambda^\alpha \theta_2 \varphi_1 \varphi_2 + f(I^*) [((\theta_2 - b_1^\alpha) (\theta_2 + b_1^\alpha) + \theta_1^2) f(I^*) + 2r^\alpha b_2^\alpha S^* f'(I^*)].$$

Since $f(I^*) > 0$ and $f(I^*) > S^* f'(I^*)$, it can be obtained that

$$2r^\alpha b_2^\alpha S^* f'(I^*) \leq ((\theta_2 - b_1^\alpha) (\theta_2 + b_1^\alpha) + \theta_1^2) f(I^*).$$

Therefore, if $\mathcal{R}_0 \leq 2$ holds, one has $g_4 > 0$. Through calculation, it can be found that

$$h_2 h_6 - h_4 h_5 \geq (\theta_1 \theta_2 (\theta_1 + \theta_2) - b_1^{2\alpha} \theta_1 - r^\alpha b_1^\alpha b_2^\alpha) f'^2(I^*) + \Lambda^{2\alpha} \theta_1^2 \theta_2 \varphi_1^2 + \Lambda^\alpha f(I^*) (2\theta_1 \theta_3 - r b_2^2) \theta_2 \varphi_1 \varphi_2 + \Lambda^{2\alpha} \theta_1 \theta_2^2 \varphi_1^2 \varphi_3 + f(I^*) \theta_1 (\theta_1 (\theta_2 - b_1^\alpha) - r^\alpha b_2^\alpha) \theta_2 \varphi_2 + \Lambda^\alpha \theta_1^2 \theta_2^2 \varphi_1 \varphi_3.$$

Further, one has $g_5 > 0$ if $\mathcal{R}_0 \leq 2$ holds. Similarly, through calculation, it can be obtained that

$$g_6 \geq [\theta_1^2 \theta_2^2 - (b_1^\alpha \theta_1 + r^\alpha b_2^\alpha)^2] f^2(I^*) + 2\Lambda^\alpha f(I^*) \theta_1^2 \theta_2 (\theta_2 - b_1^\alpha) \varphi_1 + \Lambda^\alpha \theta_1^2 \theta_2 \varphi_1 (2b_1^\alpha \varphi_2 + \Lambda^\alpha \theta_2 \varphi_1 \varphi_3).$$

Obviously, if the condition $\mathcal{R}_0 \leq 2$ holds, one has $g_6 > 0$.

In summary, if $\mathcal{R}_0 \leq 2$ holds, it can be concluded that $g_i > 0$ ($i = 2, 3, 4, 5, 6$). Therefore, the proof of Theorem 4 is completed. □

4 Bifurcation analysis

Selecting time delay τ as the bifurcation parameter, the Hopf bifurcation of model (1) is analyzed. In addition, the Hopf bifurcation of model (2) with delayed feedback control is also discussed.

4.1 Bifurcation analysis of uncontrolled model

For convenience, the following assumptions are given:

- (P1) $g_6 < 0, g_i > 0 (i = 2, 3, 4, 5)$.
- (P2) $k_1 > 0, k_3 > 0, k_1 k_2 > k_3$.

Notice that $g_1 = 2h_1 \cos(\alpha\pi/2) > 0$ for $\alpha \in (0, 1)$. It can be obviously obtained from (7) that $W'(\omega) > 0$ and $\lim_{\omega \rightarrow \infty} W(\omega) = \infty$ under assumption (P1). Further, for the equation $W(\omega) = 0$, there exists a unique positive root denoted by ω_0 . It can be deduced from (6) that

$$\tau^j = \frac{1}{\omega_0} \left[\arccos\left(\frac{-c_1 c_3 - c_2 c_4}{c_1^2 + c_2^2}\right) + 2j\pi \right], \quad j = 0, 1, 2, \dots$$

Therefore, if assumption (P1) holds, for the characteristic equation $H(\lambda) = 0$, there exists a pair of pure imaginary roots $\pm\omega_0$ at $\tau = \tau^j$. Define $\tau_0 = \min\{\tau^j\} (j = 0, 1, 2, \dots)$. Differentiating both sides of the characteristic equation $H(\lambda) = 0$ with respect to τ , one has

$$\frac{d\lambda}{d\tau} = \frac{Q_1(\lambda)}{Q_2(\lambda)},$$

where

$$\begin{aligned} Q_1(\lambda) &= (h_3\lambda^{2\alpha+1} + h_4\lambda^{\alpha+1} + h_5\lambda)e^{-\lambda\tau}, \\ Q_2(\lambda) &= 3\alpha\lambda^{3\alpha-1} + 2\alpha h_1\lambda^{2\alpha-1} + \alpha h_2\lambda^{\alpha-1} + 2\alpha h_3\lambda^{2\alpha-1}e^{-\lambda\tau} \\ &\quad - \tau h_3\lambda^{2\alpha}e^{-\lambda\tau} + \alpha h_4\lambda^{\alpha-1}e^{-\lambda\tau} - \tau h_4\lambda^\alpha e^{-\lambda\tau} - \tau h_5e^{-\lambda\tau}. \end{aligned}$$

Let $\varrho_1 = \omega_0\tau_0 - \alpha\pi$ and $\varrho_2 = \omega_0\tau_0 - \alpha\pi/2$. Define

$$\begin{aligned} q_1 &= \operatorname{Re}(Q_1(\lambda))\Big|_{\tau=\tau_0, \omega=\omega_0}, & q_2 &= \operatorname{Im}(Q_1(\lambda))\Big|_{\tau=\tau_0, \omega=\omega_0}, \\ q_3 &= \operatorname{Re}(Q_2(\lambda))\Big|_{\tau=\tau_0, \omega=\omega_0}, & q_4 &= \operatorname{Im}(Q_2(\lambda))\Big|_{\tau=\tau_0, \omega=\omega_0}. \end{aligned}$$

By calculation, it can be deduced that

$$\operatorname{Re}\left(\frac{d\lambda}{d\tau}\right)\Big|_{\tau=\tau_0, \omega=\omega_0} = \operatorname{Re}\left(\frac{Q_1(\lambda)}{Q_2(\lambda)}\right)\Big|_{\tau=\tau_0, \omega=\omega_0} = \frac{q_1 q_3 + q_2 q_4}{q_3^2 + q_4^2},$$

where

$$\begin{aligned} q_1 &= h_3\omega_0^{2\alpha+1} \sin \varrho_1 + h_4\omega_0^{\alpha+1} \sin \varrho_2 + h_5\omega_0 \sin(\omega_0\tau_0), \\ q_2 &= h_3\omega_0^{2\alpha+1} \cos \varrho_1 + h_4\omega_0^{\alpha+1} \cos \varrho_2 + h_5\omega_0 \cos(\omega_0\tau_0), \\ q_3 &= 3\alpha\omega_0^{3\alpha-1} \sin \frac{3\alpha\pi}{2} + 2\alpha h_1\omega_0^{2\alpha-1} \sin(\alpha\pi) + \alpha h_2\omega_0^{\alpha-1} \sin \frac{\alpha\pi}{2} - 2\alpha h_3\omega_0^{2\alpha-1} \sin \varrho_1 \\ &\quad - \tau_0 h_3\omega_0^{2\alpha} \cos \varrho_1 - \alpha h_4\omega_0^{\alpha-1} \sin \varrho_2 - \tau_0 h_4\omega_0^\alpha \cos \varrho_2 - \tau_0 h_5 \cos(\omega_0\tau_0), \\ q_4 &= -3\alpha\omega_0^{3\alpha-1} \cos \frac{3\alpha\pi}{2} - 2\alpha h_1\omega_0^{2\alpha-1} \cos(\alpha\pi) - \alpha h_2\omega_0^{\alpha-1} \cos \frac{\alpha\pi}{2} \\ &\quad - 2\alpha h_3\omega_0^{2\alpha-1} \cos \varrho_1 + \tau_0 h_3\omega_0^{2\alpha} \sin \varrho_1 - \alpha h_4\omega_0^{\alpha-1} \cos \varrho_2 + \tau_0 h_4\omega_0^\alpha \sin \varrho_2 \\ &\quad + \tau_0 h_5 \sin(\omega_0\tau_0). \end{aligned}$$

For convenience, the following assumption is given:

$$(P3) \quad q_1q_3 + q_2q_4 \neq 0.$$

Theorem 5. *Assuming that condition (P1) holds, it can be concluded the following:*

- (i) *For the characteristic equation $H(\lambda) = 0$, there exists a pair of pure imaginary roots $\pm\omega_0$ at $\tau = \tau^j$.*
- (ii) *Suppose that $\lambda(\tau) = \xi(\tau) + i\omega(\tau)$ is a root of the characteristic equation $H(\lambda) = 0$ near $\tau = \tau^j$ satisfying $\xi(\tau^j) = 0$ and $\omega(\tau^j) = \omega_0$. If condition (P3) holds, then we have $\text{Re}(d\lambda/d\tau)|_{\tau = \tau_0} = \omega = \omega_0 \neq 0$.*

Theorem 6. *If assumptions (P1), (P2), and (P3) hold, the following results can be obtained:*

- (i) *The endemic equilibrium point E^* of model (1) is asymptotically stable for $\tau \in [0, \tau_0)$.*
- (ii) *Model (1) undergoes a Hopf bifurcation at $\tau = \tau_0$, and it has a branch of periodic solutions bifurcation from the endemic equilibrium point E^* near $\tau = \tau_0$.*

Remark 2. According to the previous analysis, assumption (P1) in Theorem 6 can guarantee that formula (7) has a unique positive root. In fact, it only need to ensure that for (7), there exists a positive root rather than that the root is unique. If condition (P1) is reduced to $g_6 < 0$, Theorem 6 still holds.

4.2 Bifurcation analysis of controlled model

In this section, the delayed feedback controller is designed and applied to the uncontrolled model (1), which can be expressed as model (2). Adopting similar discussion, the corresponding characteristic equation corresponding to model (2) at E^* is

$$U(\lambda) = (\lambda^{3\alpha} + u_1\lambda^{2\alpha} + u_2\lambda^\alpha + u_8)e^{\lambda\tau} + (u_4\lambda^\alpha + u_6)e^{-\lambda\tau} + u_3\lambda^{2\alpha} + u_5\lambda^\alpha + u_7 = 0,$$

where

$$\begin{aligned} u_1 &= -(n_{11} + n_{22} + n_{33} + \sigma), \\ u_2 &= (n_{11} + \sigma)n_{22} + n_{22}n_{33} + (n_{11} + \sigma)n_{33}, \\ u_3 &= \sigma - p_{22}, \quad u_4 = -\sigma p_{22}, \\ u_5 &= (n_{11} + \sigma)p_{22} - \sigma n_{22} + p_{22}n_{33} - \sigma n_{33} - n_{12}p_{21}, \\ u_6 &= \sigma p_{22}n_{33}, \\ u_7 &= \sigma n_{22}n_{33} + n_{12}p_{21}n_{33} - n_{13}n_{32}p_{21} - (n_{11} + \sigma)p_{22}n_{33}, \\ u_8 &= -(n_{11} + \sigma)n_{22}n_{33}. \end{aligned}$$

For $\tau = 0$, the endemic equilibrium E^* of model (2) is locally asymptotically stable if assumption (P2) holds. It is assumed that $\lambda = \omega i$ is a purely imaginary root of $U(\lambda) = 0$, which yields

$$\begin{aligned} (v_1 + v_2) \cos(\omega\tau) + (v_3 + v_4) \sin(\omega\tau) &= v_5, \\ (v_1 - v_2) \sin(\omega\tau) + (v_4 - v_3) \cos(\omega\tau) &= v_6, \end{aligned} \tag{8}$$

where

$$\begin{aligned}
 v_1 &= \omega^{3\alpha} \cos \frac{3\alpha\pi}{2} + u_1\omega^{2\alpha} \cos(\alpha\pi) + u_2\omega^\alpha \cos \frac{\alpha\pi}{2} + u_8, \\
 v_2 &= u_4\omega^\alpha \cos \frac{\alpha\pi}{2} + u_6, \\
 v_3 &= -\omega^{3\alpha} \sin \frac{3\alpha\pi}{2} - u_1\omega^{2\alpha} \sin(\alpha\pi) - u_2\omega^\alpha \sin \frac{\alpha\pi}{2}, \\
 v_4 &= u_4\omega^\alpha \sin \frac{\alpha\pi}{2}, \quad v_5 = -u_3\omega^{2\alpha} \cos(\alpha\pi) - u_5\omega^\alpha \cos \frac{\alpha\pi}{2} - u_7, \\
 v_6 &= -u_3\omega^{2\alpha} \sin(\alpha\pi) - u_5\omega^\alpha \sin \frac{\alpha\pi}{2}.
 \end{aligned}$$

It can be calculated from formula (8) that

$$\Phi(\omega) = \omega^{12\alpha} + \Phi_1(\omega) + \rho = 0,$$

where $\Phi_1(\omega)$ is a polynomial containing $\omega^{j\alpha}$ ($j = 1, 2, \dots, 11$), and

$$\rho = u_6^4 + 2u_6u_8u_7^2 - 2u_6^2u_8^2 - u_7^2u_8^2 - u_6^2u_7^2$$

is a constant. Supposing $\rho < 0$, the equation $\Phi(\omega) = 0$ admits at least one positive real root, which is defined by $\bar{\omega}_0$. Then we can obtain

$$\bar{\tau}^j = \frac{1}{\bar{\omega}_0} \left\{ \arccos \left[\frac{(v_1 - v_2)v_5 - (v_3 + v_4)v_6}{v_1^2 + v_3^2 - v_2^2 - v_4^2} \right] + 2j\pi \right\}, \quad j = 0, 1, 2, \dots$$

Define the bifurcation point $\bar{\tau}_0 = \min\{\bar{\tau}^j\}$, ($j = 0, 1, 2, \dots$). Differentiating both sides of the characteristic equation $U(\lambda) = 0$ with respect to τ , one has

$$\frac{d\lambda}{d\tau} = \frac{\bar{Q}_1(\lambda)}{\bar{Q}_2(\lambda)},$$

where

$$\bar{Q}_1(\lambda) = \zeta_1(\lambda) + \zeta_2(\lambda)e^{-2\lambda\tau}, \quad \bar{Q}_2(\lambda) = \zeta_3(\lambda) + \zeta_4(\lambda)e^{-\lambda\tau} + \zeta_5(\lambda)e^{-2\lambda\tau}$$

with

$$\begin{aligned}
 \zeta_1(\lambda) &= -\lambda^{3\alpha+1} - u_1\lambda^{2\alpha+1} - u_2\lambda^{\alpha+1} - u_8\lambda, & \zeta_2(\lambda) &= u_4\lambda^{\alpha+1} + u_6\lambda, \\
 \zeta_3(\lambda) &= 3\alpha\lambda^{3\alpha-1} + \tau\lambda^{3\alpha} + 2\alpha u_1\lambda^{2\alpha-1} + \tau u_1\lambda^{2\alpha} + \alpha u_2\lambda^{\alpha-1} + \tau u_2\lambda^\alpha + \tau u_8, \\
 \zeta_4(\lambda) &= \alpha u_5\lambda^{\alpha-1} + 2\alpha u_3\lambda^{2\alpha-1}, & \zeta_5(\lambda) &= \alpha u_4\lambda^{\alpha-1} - \tau u_4\lambda^\alpha - \tau u_6.
 \end{aligned}$$

Let $\bar{q}_1 = \alpha\pi/2 - 2\bar{\omega}_0\bar{\tau}_0$, $\bar{q}_2 = \alpha\pi - \bar{\omega}_0\bar{\tau}_0$, and $\bar{q}_3 = \alpha\pi/2 - \bar{\omega}_0\bar{\tau}_0$. Define

$$\begin{aligned}
 \bar{q}_1 &= \text{Re}(\bar{Q}_1(\lambda)) \Big|_{\tau=\bar{\tau}_0, \omega=\bar{\omega}_0}, & \bar{q}_2 &= \text{Im}(\bar{Q}_1(\lambda)) \Big|_{\tau=\bar{\tau}_0, \omega=\bar{\omega}_0}, \\
 \bar{q}_3 &= \text{Re}(\bar{Q}_2(\lambda)) \Big|_{\tau=\bar{\tau}_0, \omega=\bar{\omega}_0}, & \bar{q}_4 &= \text{Im}(\bar{Q}_2(\lambda)) \Big|_{\tau=\bar{\tau}_0, \omega=\bar{\omega}_0}.
 \end{aligned}$$

By calculation, it can be obtained that

$$\text{Re} \left(\frac{d\lambda}{d\tau} \right) \Big|_{\tau=\bar{\tau}_0, \omega=\bar{\omega}_0} = \frac{\bar{q}_1\bar{q}_3 + \bar{q}_2\bar{q}_4}{\bar{q}_3^2 + \bar{q}_4^2},$$

where

$$\begin{aligned} \bar{q}_1 &= \bar{\omega}_0^{3\alpha+1} \sin \frac{3\alpha\pi}{2} + u_1 \bar{\omega}_0^{2\alpha+1} \sin \alpha\pi + u_2 \bar{\omega}_0^{\alpha+1} \sin \frac{\alpha\pi}{2} - u_4 \bar{\omega}_0^{\alpha+1} \sin \bar{\varrho}_1 \\ &\quad + u_4 \bar{\omega}_0 \sin(2\bar{\omega}_0 \bar{\tau}_0), \\ \bar{q}_2 &= -\bar{\omega}_0^{3\alpha+1} \cos \frac{3\alpha\pi}{2} - u_1 \bar{\omega}_0^{2\alpha+1} \cos \alpha\pi - u_2 \bar{\omega}_0^{\alpha+1} \cos \frac{\alpha\pi}{2} + u_4 \bar{\omega}_0^{\alpha+1} \cos \bar{\varrho}_1 \\ &\quad + u_4 \bar{\omega}_0 \cos(2\bar{\omega}_0 \bar{\tau}_0) - u_8 \bar{\omega}_0, \\ \bar{q}_3 &= 3\alpha \bar{\omega}_0^{3\alpha-1} \sin \frac{3\alpha\pi}{2} + \bar{\tau}_0 \bar{\omega}_0^{3\alpha} \cos \frac{3\alpha\pi}{2} + 2\alpha u_1 \bar{\omega}_0^{2\alpha-1} \sin \alpha\pi + u_1 \bar{\tau}_0 \bar{\omega}_0^{2\alpha} \cos(\alpha\pi) \\ &\quad + \alpha u_2 \bar{\omega}_0^{\alpha-1} \sin \frac{\alpha\pi}{2} + u_2 \bar{\tau}_0 \bar{\omega}_0^\alpha \cos \frac{\alpha\pi}{2} + 2\alpha u_3 \bar{\omega}_0^{2\alpha-1} \sin \bar{\varrho}_2 + \alpha u_4 \bar{\omega}_0^{\alpha-1} \sin \bar{\varrho}_1 \\ &\quad - u_4 \bar{\tau}_0 \bar{\omega}_0^\alpha \cos \bar{\varrho}_1 + \alpha u_5 \bar{\tau}_0 \bar{\omega}_0^{\alpha-1} \sin \bar{\varrho}_3 - u_6 \bar{\tau}_0 \cos(2\bar{\omega}_0 \bar{\tau}_0) + u_8 \bar{\tau}_0, \\ \bar{q}_4 &= -3\alpha \bar{\omega}_0^{3\alpha-1} \cos \frac{3\alpha\pi}{2} + \bar{\tau}_0 \bar{\omega}_0^{3\alpha} \sin \frac{3\alpha\pi}{2} - 2\alpha u_1 \bar{\omega}_0^{2\alpha-1} \cos \alpha\pi + u_1 \bar{\tau}_0 \bar{\omega}_0^{2\alpha} \sin(\alpha\pi) \\ &\quad - \alpha u_2 \bar{\omega}_0^{\alpha-1} \cos \frac{\alpha\pi}{2} + u_2 \bar{\tau}_0 \bar{\omega}_0^\alpha \sin \frac{\alpha\pi}{2} - 2\alpha u_3 \bar{\omega}_0^{2\alpha-1} \cos \bar{\varrho}_2 - \alpha u_4 \bar{\omega}_0^{\alpha-1} \cos \bar{\varrho}_1 \\ &\quad - u_4 \bar{\tau}_0 \bar{\omega}_0^\alpha \sin \bar{\varrho}_1 - \alpha u_5 \bar{\tau}_0 \bar{\omega}_0^{\alpha-1} \cos \bar{\varrho}_3 + u_6 \bar{\tau}_0 \sin(2\bar{\omega}_0 \bar{\tau}_0). \end{aligned}$$

For convenience, the following assumptions are given:

(P4) $\rho = u_6^4 + 2u_6 u_8 u_7^2 - 2u_6^2 u_8^2 - u_7^2 u_8^2 - u_6^2 u_7^2 < 0.$

(P5) $\bar{q}_1 \bar{q}_3 + \bar{q}_2 \bar{q}_4 \neq 0.$

Theorem 7. Assuming that condition (P4) holds, the following results are drawn:

- (i) For the characteristic equation $U(\lambda) = 0$, there exists a pair of pure imaginary roots $\pm \bar{\omega}_0$ at $\tau = \bar{\tau}^j$.
- (ii) Suppose that $\lambda(\tau) = \xi(\tau) + i\omega(\tau)$ is a root of the characteristic equation $U(\lambda) = 0$ near $\tau = \bar{\tau}^j$ satisfying $\xi(\bar{\tau}^j) = 0$ and $\omega(\bar{\tau}^j) = \bar{\omega}_0$. If condition (P5) holds, then we have $\text{Re}(d\lambda/d\tau)|_\tau = \bar{\tau}_0, \omega = \bar{\omega}_0 \neq 0$.

Theorem 8. If assumptions (P2), (P4), and (P5) hold, the following results can be obtained:

- (i) The endemic equilibrium E^* of model (2) is asymptotically stable for $\tau \in [0, \bar{\tau}_0)$.
- (ii) Model (2) undergoes a Hopf bifurcation at $\tau = \bar{\tau}_0$, and it has a branch of periodic solutions bifurcation from the endemic equilibrium point E^* near $\tau = \bar{\tau}_0$.

5 Optimal control

During the prevention and control of the pandemic, there is a time interval from the formulation of control strategies to the specific implementation. Therefore, the optimal control problem of fractional-order epidemic model (1) with delayed control is discussed in this section. The common control measures are mainly to reduce the infection rate by limiting the effective contact between virus carriers and susceptible individuals. Therefore, $(1 - u)$ is selected to represent the reduction in infection rate under relevant control measures. The

corresponding DFOCP with delayed control can be described as

$$\min \mathcal{J}(u) = \int_0^{t_f} \omega_1 I(t) + \omega_2 u^2(t) dt \tag{9}$$

with the following state constraints:

$$\begin{aligned} D^\alpha S(t) &= \Lambda^\alpha S(t) \left(1 - \frac{S(t)}{K}\right) - (1-u)Sf(I) + b_1^\alpha I(t) + b_2^\alpha R(t), \\ D^\alpha I(t) &= (1-u(t-\tau))S(t-\tau)f(I(t-\tau)) - (r^\alpha + b_1^\alpha + d_1^\alpha + d_2^\alpha)I(t), \\ D^\alpha R(t) &= r^\alpha I(t) - (d_1^\alpha + b_2^\alpha)R(t), \end{aligned} \tag{10}$$

where the initial condition is the same as in model (1), formula (9) represents the performance index, ω_1 and ω_2 are weight coefficients, and the corresponding feasible control domain is $\mathcal{M} = \{u(t)|u(t) \in [0, u_{\max}], t \in [0, t_f]\}$, u_{\max} represents the maximum value of the optimal control u in the feasible control domain \mathcal{M} . The Hamiltonian function is defined as

$$\begin{aligned} \mathcal{H} &= \omega_1 I + \omega_2 u^2 + \lambda_1 \left[\Lambda^\alpha S \left(1 - \frac{S}{K}\right) - (1-u)Sf(I) + b_1^\alpha I + b_2^\alpha R \right] \\ &+ \lambda_2 \left[(1-u(t-\tau))S(t-\tau)f(I(t-\tau)) - (r^\alpha + b_1^\alpha + d_1^\alpha + d_2^\alpha)I \right] \\ &+ \lambda_3 \left[r^\alpha I - (d_1^\alpha + b_2^\alpha)R \right]. \end{aligned}$$

Define the following function:

$$\chi_{[0, t_f-\tau]} = \begin{cases} 1, & t \in [0, t_f - \tau], \\ 0, & t \notin [0, t_f - \tau]. \end{cases}$$

According to [9], the adjoint system corresponding to the Caputo fractional-order state system should be an Riemann–Liouville fractional-order system [1]. According to the optimal control principles for delayed fractional-order systems [2, 3, 9, 10, 21], the Euler–Lagrange equation for DFOCP (9)–(10) can be obtained. Therefore, the following results can be drawn.

Theorem 9. *Let u_* be the optimal control corresponding to the optimal state variables S_*, I_*, R_* in DFOCP (9)–(10). Then the corresponding adjoint system is*

$$\begin{aligned} {}^R D_{t_f}^\alpha \lambda_1(t) &= \left[\Lambda^\alpha - \frac{2\Lambda^\alpha S}{K} - (1-u)f(I) \right] \lambda_1(t) + \chi_{[0, t_f-\tau]}(1-u)f(I)\lambda_2(t+\tau), \\ {}^R D_{t_f}^\alpha \lambda_2(t) &= \omega_1 + \left[b_1^\alpha - (1-u)S \frac{\partial f(I)}{\partial I} \right] \lambda_1(t) - (r^\alpha + b_1^\alpha + d_1^\alpha + d_2^\alpha)\lambda_2(t) \\ &+ r^\alpha \lambda_3(t) + \chi_{[0, t_f-\tau]}(1-u)S \frac{\partial f(I)}{\partial I(t-\tau)} \lambda_2(t+\tau), \\ {}^R D_{t_f}^\alpha \lambda_3(t) &= b_2^\alpha \lambda_1 - (d_1^\alpha + b_2^\alpha)\lambda_3 \end{aligned} \tag{11}$$

with transversality condition ${}^R D_{t_f}^{\alpha-1} \lambda_i(t_f) = 0, i = 1, 2, 3$. The corresponding optimal control is

$$u_* = \min \left\{ \max \left\{ 0, \frac{S_* f(I_*) (\chi_{[0, t_f - \tau]} \lambda_2(t + \tau) - \lambda_1)}{2\omega_2} \right\}, u_{\max} \right\}. \tag{12}$$

Proof. According to the Pontryagin’s maximum principle and the results in [10, 21], the adjoint system corresponding to DFOCP (9)–(10) can be obtained as

$$\begin{aligned} {}^R D_{t_f}^\alpha \lambda_1(t) &= \frac{\partial \mathcal{H}}{\partial S} + \chi_{[0, t_f - \tau]} \frac{\partial H(t + \tau)}{\partial S(t - \tau)}, \\ {}^R D_{t_f}^\alpha \lambda_2(t) &= \frac{\partial \mathcal{H}}{\partial I} + \chi_{[0, t_f - \tau]} \frac{\partial H(t + \tau)}{\partial I(t - \tau)}, \quad {}^R D_{t_f}^\alpha \lambda_3(t) = \frac{\partial \mathcal{H}}{\partial R} \end{aligned}$$

with transversality condition ${}^R D_{t_f}^{\alpha-1} \lambda_i(t_f) = 0, i = 1, 2, 3$. The optimal control formula (12) can be calculated based on the feasible control domain \mathcal{M} and the following optimality condition: $\partial \mathcal{H} / \partial u + \chi_{[0, t_f - \tau]} \partial H(t + \tau) / \partial u(t - \tau) = 0$. Furthermore, according to the above equation, it can be calculated that

$$u_* = \frac{S_* f(I_*) (\chi_{[0, t_f - \tau]} \lambda_2(t + \tau) - \lambda_1)}{2\omega_2}.$$

Since the optimal control u_* remain in the feasible control domain \mathcal{M} , the optimal control is

$$u_* = \min \left\{ \max \left\{ 0, \frac{S_* f(I_*) (\chi_{[0, t_f - \tau]} \lambda_2(t + \tau) - \lambda_1)}{2\omega_2} \right\}, u_{\max} \right\}.$$

Therefore, the corresponding adjoint system and optimality condition can be derived. \square

The forward-backward sweep method (FBSM) is adopted to numerically solve DFOCP (9)–(10) with delayed control based on Theorem 9 and [9, 16]. The Riemann–Liouville fractional-order adjoint system (11) with transversality conditions can be numerically solved by the fractional predictor-corrector method [8] and the method mentioned in [9].

6 Numerical simulations

The theoretical results are verified in this section. In addition, parameters of the model are identified based on the measurement data of COVID-19 pandemic. According to the results of parameter identification, the model established in this paper is verified to be effective in depicting COVID-19 pandemic. Further, the DFOCP with delayed control is numerically analyzed.

6.1 Verification of relevant theoretical results

Assume that the state variables in model (1) represent the density of population. Then the saturated incidence rate $Sf(I) = \gamma_2 SI / (1 + \gamma_1 I)$ is selected, where γ_1 is the saturation

coefficient, γ_2 is the average number of susceptible individuals infected by per infected individual per day. Therefore, the epidemic model with saturated incidence rate based on model (2) can be expressed as

$$\begin{aligned}
 {}_0^C D_t^\alpha S(t) &= \Lambda^\alpha S(t) \left(1 - \frac{S(t)}{K} \right) - \frac{\gamma_2^\alpha S(t) I(t)}{1 + \gamma_1 I(t)} + b_1^\alpha I(t) + b_2^\alpha R(t) \\
 &\quad + \sigma(S(t) - S(t - \tau)), \\
 {}_0^C D_t^\alpha I(t) &= \frac{\gamma_2^\alpha S(t - \tau) I(t - \tau)}{1 + \gamma_1 I(t - \tau)} - (r^\alpha + b_1^\alpha + d_1^\alpha + d_2^\alpha) I(t), \\
 {}_0^C D_t^\alpha R(t) &= r^\alpha I(t) - (d_1^\alpha + b_2^\alpha) R(t),
 \end{aligned}
 \tag{13}$$

where the initial condition is the same as in model (1). When $\sigma = 0$, model (13) is a special case of model (1). According to the description of parameter γ_2 , $I(t)$ no longer simply represents the number of infected individuals, but the number of infected individuals who have been diagnosed. For convenience, $I(t)$ is described as the number of currently infected individuals.

Considering no self-feedback control, that is, $\sigma = 0$, the accuracy of the relevant theoretical results is verified. The initial value is $(S(0), I(0), R(0)) = (0.63, 0.76, 0.28)$, and the following parameters are selected: $\Lambda = 0.2$, $K = 50$, $\gamma_1 = 0.002$, $\gamma_2 = 0.07$, $b_1 = 0.006$, $b_2 = 0.05$, $r = 0.035$, $d_1 = 0.0375$, $d_2 = 0.045$, $b_2 = 0.05$. Under this set of parameters and $\sigma = 0$, it can be calculated that model (13) has an endemic equilibrium point $E^* = (1.8003, 3.4461, 1.3849)$. This set of parameters clearly satisfies the condition of conclusion (i) in Theorem 4. Therefore, the endemic equilibrium E^* is locally asymptotically stable for $\tau = 0$ as shown in Figs. 1(a) and 1(e). According to Theorem 5, it can be calculated that the bifurcation point $\tau_0 = 6.7576$ and the critical frequency $\omega_0 = 0.1151$. Through calculation, it can be found that the set of parameters selected above meet the conditions of Theorem 5. When $\tau = 2.5815 \in (0, \tau_0)$, the solution of model (13) with $\sigma = 0$ is still locally asymptotically stable as shown in Figs. 1(c) and 1(d). When the time delay $\tau = 7.8225 > \tau_0$, model (13) with $\sigma = 0$ loses its local asymptotic stability at the endemic equilibrium point E^* as shown in Figs. 1(b) and 1(f). This is consistent with the conclusion of Theorem 6.

When $\sigma = 0$, the corresponding bifurcation point and critical frequency are $\tau_0 = 6.7576$ and $\omega_0 = 0.1151$, respectively. If the latency delay $\tau = 6.8 > 6.7576 = \tau_0$, then the endemic equilibrium E^* is unstable as shown in Fig. 2(a). In order to effectively control the critical bifurcation point, the feedback coefficient $\sigma = -0.01$ is selected. The corresponding bifurcation point and critical frequency can be calculated as $\bar{\tau}_0 = 7.6192$ and $\bar{\omega}_0 = 0.1076$, respectively. The time delay $\tau = 6.8 \in (0, \bar{\tau}_0)$, the endemic equilibrium E^* is locally asymptotically stable as shown in Fig. 2(b). The latent delay further increases to $\tau = 7.8 > 7.6192 = \bar{\tau}_0$, and the endemic equilibrium E^* is unstable as shown in Fig. 2(c). Letting $\sigma = -0.02$, the condition of Theorem 8 is still hold. Then the corresponding bifurcation point and critical frequency are $\bar{\tau}_0 = 8.9677$ and $\bar{\omega}_0 = 0.09832$, respectively. The latent delay $\tau = 7.8 \in (0, \bar{\tau}_0)$, according to Theorem 8, it can be obtained that the endemic equilibrium E^* once again tends to be locally asymptotically stable as shown in Fig. 2(d). The above analysis provides

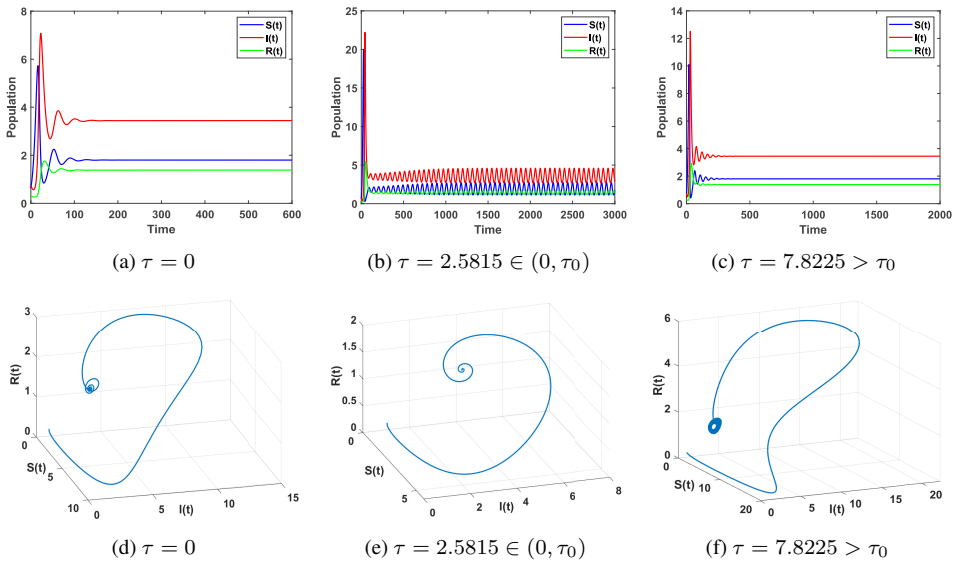


Figure 1. The curve of model (13) with $\sigma = 0$.

support for the accuracy of the conclusion of Theorem 8. Meanwhile, it also shows that adding appropriate delayed feedback controller can make model (13) obtain better dynamic characteristics.

6.2 Application of optimal control to the COVID-19 pandemic

In Tables 3–6 of [25], it can be found that compared to the corresponding integer-order epidemic model (order $\alpha = 1$), the Caputo fractional-order epidemic model can better predict the short-term trend of COVID-19. In Figs. 2, 3 and Table 1 of [19], it can be observed that compared to integer-order epidemic model, the Caputo fractional-order epidemic model can better fit the trend of COVID-19.

In this section, the saturated incidence rate is used to describe the trend of COVID-19 pandemic. In order to fit the type of COVID-19 data, $S(t)$, $I(t)$, and $R(t)$ in model (1) are all expressed as the number of individuals at time t . Therefore, the corresponding saturated incidence rate can be described as $Sf(I) = \gamma_2 SI / (N_p + \gamma_1 I)$, where N_p represents the total population. Therefore, the corresponding model describing the COVID-19 pandemic can be written as

$$\begin{aligned}
 {}_0^C D_t^\alpha S(t) &= \Lambda^\alpha S(t) \left(1 - \frac{S(t)}{K} \right) - \frac{\gamma_2^\alpha S(t) I(t)}{N_p + \gamma_1 I(t)} + b_1^\alpha I(t) + b_2^\alpha R(t), \\
 {}_0^C D_t^\alpha I(t) &= \frac{\gamma_2^\alpha S(t - \tau) I(t - \tau)}{N_p + \gamma_1 I(t - \tau)} - (r^\alpha + b_1^\alpha + d_1^\alpha + d_2^\alpha) I(t), \\
 {}_0^C D_t^\alpha R(t) &= r^\alpha I(t) - (d_1^\alpha + b_2^\alpha) R(t).
 \end{aligned}
 \tag{14}$$

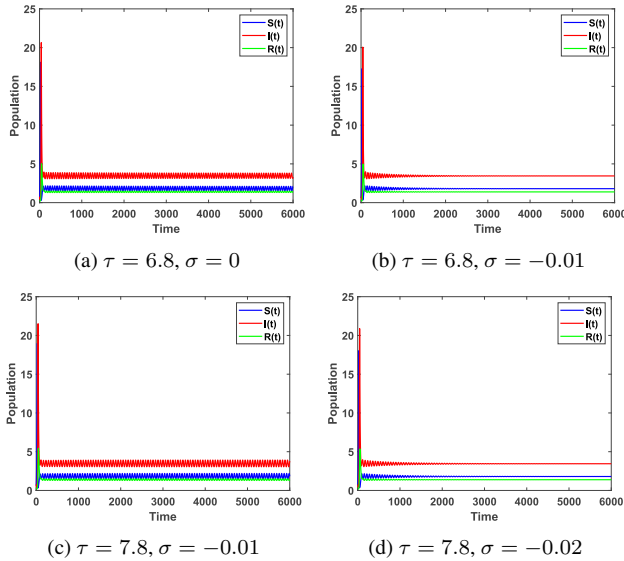


Figure 2. The effect diagram of the delayed feedback controller on bifurcation control.

In addition, the commonly used data on the COVID-19 pandemic mainly fall into three categories: cumulative confirmed cases, recovered cases, and death cases. Based on the above three types of data, the number of currently infected individuals can be measured. The relevant data of the COVID-19 pandemic used in this paper are provided by World Health Organization (<https://www.who.int>) and Worldometer (<https://www.worldometers.info>). The measurement data during the COVID-19 outbreak in Brazil are selected to identify the parameters of model (14). The average life expectancy of Brazil is 76.18, then the natural mortality rate is $d_1 = 1/(76.18 \cdot 365) = 3.5964 \cdot 10^{-5}$. Assume that the incubation period of COVID-19 is $\tau = 2$. In addition, based on the data of cumulative recovered cases and cumulative death cases, the daily recovery rate and daily death rate can be determined. Assuming that the recovery rate r and death rate d_2 are the average of daily recovery rate and daily death rate, the recovery rate $r = 0.0581$ and death rate $d_2 = 3.4114 \cdot 10^{-4}$ can be calculated. Further, the initial value of currently infected individuals is $I(0) = 104523$. The initial values for recovered individuals and susceptible individuals are $R(0) = 0.1(N_p - I(0)) \approx 2.1521 \cdot 10^7$ and $S(0) = 0.5(N_p - I(0) - R(0)) \approx 9.6844 \cdot 10^7$, respectively. The data of the currently infected individuals is selected to identify other parameters of model (14). The least squares fitting method is adopted to identify the parameters of model (14). Specifically, the minimization objective function is considered as $J_{\min} = \sum_{i=1}^n (Q_m(i) - Q_c(i))^2$, where $Q_m(i)$ and $Q_c(i)$ represent the measurement data and fitting data of the currently infected individuals on day i . The results of parameter identification are shown in Table 1. In addition, the fitting effect of model (14) on the COVID-19 data is shown in Fig. 3(d).

Figure 3(a) shows that model (14) can effectively depict the trend of COVID-19 pandemic. Under the above parameters, it can be calculated that the conditions $l_1 > 0$,

Table 1. Parameter identification.

Parameter	Value	Parameter	Value
Λ	$0.0032 \text{ (day)}^{-1}$	b_1	$0.8955 \text{ (day)}^{-1}$
K	$1.7633 \cdot 10^7 \text{ persons}$	b_2	$0.1149 \text{ (day)}^{-1}$
γ_1	4.9262	α	0.9996
γ_2	$3.1902 \text{ (person)}^{-1} \cdot \text{(day)}^{-1}$		

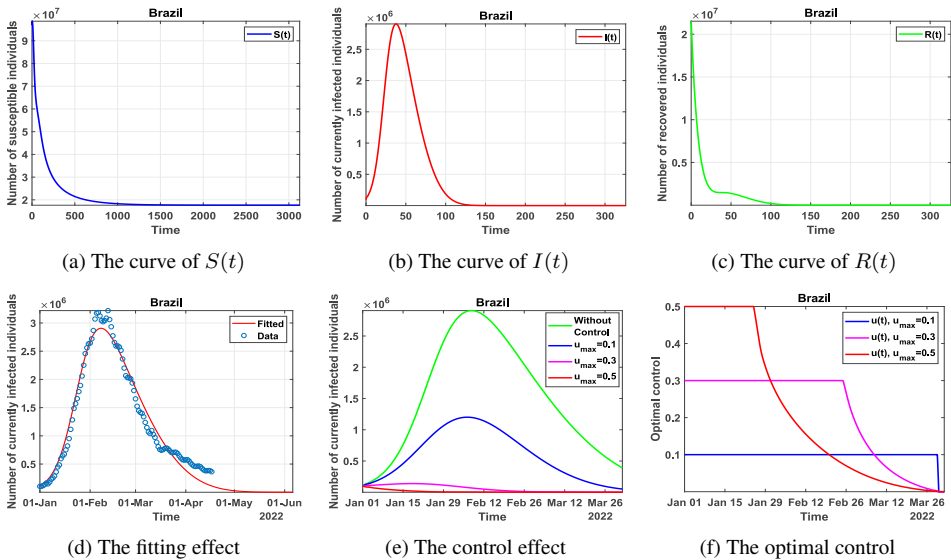


Figure 3. The fitting effect and optimal control.

$l_3 > 0$, $l_1 l_2 > l_3$, and $f_i > 0$ ($i = 2, 3, 4, 5, 6$) hold, which satisfies the conditions of Theorem 3. According to the result of Theorem 3, the disease-free equilibrium $E_1 = (1.763 \cdot 10^7, 0, 0)$ of model (14) should be locally asymptotically stable as shown in Figs. 3(a)–3(c).

Based on model (14), the corresponding DFOCP can be described as

$$\min \mathcal{J}(u) = \int_0^{t_f} \omega_1 I(t) + \omega_2 u^2(t) dt \tag{15}$$

with the following state constraints:

$$\begin{aligned} {}_0^C D_t^\alpha S(t) &= \Lambda^\alpha S \left(1 - \frac{S}{K} \right) - \frac{(1-u)\gamma_2^\alpha SI}{N_p + \gamma_1 I} + b_1^\alpha I + b_2^\alpha R, \\ {}_0^C D_t^\alpha I(t) &= \frac{(1-u(t-\tau))\gamma_2^\alpha S(t-\tau)I(t-\tau)}{N_p + \gamma_1 I(t-\tau)} - (r^\alpha + b_1^\alpha + d_1^\alpha + d_2^\alpha)I, \\ {}_0^C D_t^\alpha R(t) &= r^\alpha I - (d_1^\alpha + b_2^\alpha)R. \end{aligned} \tag{16}$$

According to Theorem 9, the adjoint system, transversality condition, and optimal control can be obtained. Based on the parameters in Table 1, the FBSM method is adopted to numerically solve DFOCP (15)–(16). Select the weight coefficient $\omega_1 = 1$ and $\omega_2 = 10^5$. The control measures will be implemented for 90 days from January 1, 2022. In DFOCP (15)–(16), the larger the value of u_{\max} , the better the optimal control effect, which is shown in Figs. 3(e) and 3(f). It can be found that the implementation of the optimal control strategy can greatly reduce the number of infected individuals in a short time, which can quickly control the pandemic.

7 Conclusions

The purpose of this paper is to provide theoretical guidance for the effective control of outbreaks through the fractional-order epidemic model. Considering the universality of the incubation period of pathogens and the diversity of incidence rates, a delayed fractional-order SIRS model with general incidence rate is established. In order to capture better dynamic behaviors regarding Hopf bifurcation, feedback control with time delay is adopted to the model. The Hopf bifurcation of uncontrolled model and controlled model is theoretically analyzed.

The parameters of the model are identified through the measurement data of COVID-19 pandemic. By selecting appropriate control strategies, the DFOCP with delayed control is proposed. The FBSM is adopted to numerically solve the DFOCP with delayed control. The corresponding results of numerical simulation show that the optimal control strategy can quickly and effectively control the trend of the epidemic.

References

1. T. Abdeljawad, A. Atangana, J.F. Gómez-Aguilar, F. Jarad, On a more general fractional integration by parts formulae and applications, *Physica A*, **536**:122494, 2019, <https://doi.org/10.1016/j.physa.2019.122494>.
2. O.P. Agrawal, Formulation of Euler–Lagrange equations for fractional variational problems, *J. Math. Anal. Appl.*, **272**(1):368–379, 2002, [https://doi.org/10.1016/S0022-247X\(02\)00180-4](https://doi.org/10.1016/S0022-247X(02)00180-4).
3. O.P. Agrawal, A general formulation and solution scheme for fractional optimal control problems, *Nonlinear Dyn.*, **38**:323–337, 2004, <https://doi.org/10.1007/s11071-004-3764-6>.
4. J. Alidousti, M.M. Ghahfarokhi, Stability and bifurcation for time delay fractional predator prey system by incorporating the dispersal of prey, *Appl. Math. Model.*, **72**:385–402, 2019, <https://doi.org/10.1016/j.apm.2019.03.029>.
5. V. Capasso, G. Serio, A generalization of the Kermack–McKendrick deterministic epidemic model, *Math. Biosci.*, **42**(1–2):43–61, 1978, [https://doi.org/10.1016/0025-5564\(78\)90006-8](https://doi.org/10.1016/0025-5564(78)90006-8).
6. W.H. Deng, C.P. Li, J.H. Lü, Stability analysis of linear fractional differential system with multiple time delays, *Nonlinear Dyn.*, **48**:409–416, 2007, <https://doi.org/10.1007/s11071-006-9094-0>.

7. K. Diethelm, A fractional calculus based model for the simulation of an outbreak of dengue fever, *Nonlinear Dyn.*, **71**(4):613–619, 2013, <https://doi.org/10.1007/s11071-012-0475-2>.
8. K. Diethelm, N.J. Ford, A.D. Freed, A predictor-corrector approach for the numerical solution of fractional differential equations, *Nonlinear Dyn.*, **29**(1–4):3–22, 2002, <https://doi.org/10.1023/A:1016592219341>.
9. Y.S. Ding, Z.D. Wang, H.P. Ye, Optimal control of a fractional-order HIV-immune system with memory, *IEEE Trans. Control Syst. Technol.*, **20**(3):763–769, 2012, <https://doi.org/10.1109/TCST.2011.2153203>.
10. S. Effati, S.A. Rakhshan, S. Saqi, Formulation of Euler–Lagrange equations for multidelay fractional optimal control problems, *J. Comput. Nonlinear Dyn.*, **13**(6):061007, 2018, <https://doi.org/10.1115/1.4039900>.
11. N. Hamdan, A. Kilicman, A fractional order sir epidemic model for dengue transmission, *Chaos Solitons Fractals*, **114**:55–62, 2018, <https://doi.org/10.1016/j.chaos.2018.06.031>.
12. C.D. Huang, J.D. Cao, M. Xiao, A. Alsaedi, F.E. Alsaadi, Controlling bifurcation in a delayed fractional predator–prey system with incommensurate orders, *Appl. Math. Comput.*, **293**:293–310, 2017, <https://doi.org/10.1016/j.amc.2016.08.033>.
13. C.D. Huang, H. Li, J.D. Cao, A novel strategy of bifurcation control for a delayed fractional predator–prey model, *Appl. Math. Comput.*, **347**:808–838, 2019, <https://doi.org/10.1016/j.amc.2018.11.031>.
14. Y. Jalilian, R. Jalilian, Existence of solution for delay fractional differential equations, *Mediterr. J. Math.*, **10**(4):1731–1747, 2013, <https://doi.org/10.1007/s00009-013-0281-1>.
15. W.O. Kermack, A.G. McKendrick, A contribution to the mathematical theory of epidemics, *Proc. R. Soc. Lond.*, **115**(772):700–721, 1927, <https://doi.org/10.1098/rspa.1927.0118>.
16. S. Lenhart, J.T. Workman, *Optimal Control Applied to Biological Models*, CRC Press, London, 2007.
17. C.P. Li, Y.T. Ma, Fractional dynamical system and its linearization theorem, *Nonlinear Dyn.*, **71**(4):621–633, 2013, <https://doi.org/10.1007/s11071-012-0601-1>.
18. T. Li, F.Q. Zhang, H.W. Liu, Y.M. Chen, Threshold dynamics of an SIRS model with nonlinear incidence rate and transfer from infectious to susceptible, *Appl. Math. Lett.*, **70**:52–27, 2017, <https://doi.org/10.1016/j.aml.2017.03.005>.
19. Z.Z. Lu, Y.G. Yu, Y.Q. Chen, C.H. Xu, S.H. Wang, Z. Yin, A fractional-order SEIHDR model for COVID-19 with inter-city networked coupling effects, *Nonlinear Dyn.*, **101**(3):1717–1730, 2020, <https://doi.org/10.1007/s11071-020-05848-4>.
20. I. Podlubny, *Fractional Differential Equations*, Academic Press, New York, 1999.
21. S.A. Rakhshan, S. Effati, Fractional optimal control problems with time-varying delay: A new delay fractional Euler–Lagrange equations, *J. Franklin Inst.*, **357**(10):5954–5988, 2020, <https://doi.org/10.1016/j.jfranklin.2020.03.038>.
22. S. Ruan, W. Wang, Dynamical behavior of an epidemic model with a nonlinear incidence rate, *J. Differ. Equations*, **188**(1):135–163, 2003, [https://doi.org/10.1016/S0022-0396\(02\)00089-X](https://doi.org/10.1016/S0022-0396(02)00089-X).

23. P. van den Driessche, J. Watmough, Reproduction numbers and sub-threshold endemic equilibria for compartmental models of disease transmission, *Math. Biosci.*, **180**:29–48, 2002, [https://doi.org/10.1016/S0025-5564\(02\)00108-6](https://doi.org/10.1016/S0025-5564(02)00108-6).
24. H. Wang, Y.G. Yu, G.G. Wen, S. Zhang, J.Z. Yu, Global stability analysis of fractional-order Hopfield neural networks with time delay, *Neurocomputing*, **154**:15–23, 2015, <https://doi.org/10.1016/j.neucom.2014.12.031>.
25. C.H. Xu, Y.G. Yu, Y.Q. Chen, Z.Z. Lu, Forecast analysis of the epidemics trend of COVID-19 in the USA by a generalized fractional-order SEIR model, *Nonlinear Dyn.*, **101**(3):1621–1634, 2020, <https://doi.org/10.1007/s11071-020-05946-3>.
26. R. Xu, Z.E. Ma, Global stability of a delayed SEIRS epidemic model with saturation incidence rate, *Nonlinear Dyn.*, **61**(1–2):229–239, 2010, <https://doi.org/10.1007/s11071-009-9644-3>.
27. R. Xu, Z.E. Ma, Z.P. Wang, Global stability of a delayed SIRS epidemic model with saturation incidence and temporary immunity, *Comput. Math. Appl.*, **59**(9):3211–3221, 2010, <https://doi.org/10.1016/j.camwa.2010.03.009>.
28. J.Y. Zhou, Y. Ye, A. Arenas, S. Gómez, Y. Zhao, Pattern formation and bifurcation analysis of delay induced fractional-order epidemic spreading on networks, *Chaos Solitons Fractals*, **174**: 113805, 2023, <https://doi.org/10.1016/j.chaos.2023.113805>.
29. J.Y. Zhou, Y. Zhao, Y. Ye, Y.X. Bao, Bifurcation analysis of a fractional-order simplicial SIRS system induced by double delays, *Int. J. Bifurcation Chaos Appl. Sci. Eng.*, **32**(5):2250068, 2022, <https://doi.org/10.1142/S0218127422500687>.
30. X.Y. Zhou, M.Y. Wang, Dynamic analysis of a fractional-order SIRS model with time delay, *Nonlinear Anal. Model. Control*, **27**(2):368–384, 2022, <https://doi.org/10.15388/namc.2022.27.26296>.